

---

## Research Article

Theme: Lipid-Based Drug Delivery Strategies for Oral Drug Delivery  
Guest Editor: Sanyog Jain

---

# Development and Characterization of a Self-Nanoemulsifying Drug Delivery System Comprised of Rice Bran Oil for Poorly Soluble Drugs

Georgios K. Eleftheriadis,<sup>1</sup> Panagiota Mantelou,<sup>1</sup> Christina Karavasili,<sup>1</sup> Paschalina Chatzopoulou,<sup>2</sup> Dimitrios Katsantonis,<sup>3</sup> Maria Irakli,<sup>2</sup> Aggeliki Mygdalia,<sup>3</sup> Ioannis S. Vizirianakis,<sup>4</sup> and Dimitrios G. Fatouros<sup>1,5</sup>

Received 30 August 2018; accepted 11 December 2018; published online 11 January 2019

**Abstract.** Poor aqueous solubility and low bioavailability are limiting factors in the oral delivery of lipophilic drugs. In a formulation approach to overcome these limitations, rice bran (RB) oil was evaluated as drug carrier in the development of self-nanoemulsifying drug delivery systems (SNEDDS). The performance of RB in formulations incorporating Kolliphor RH40 or Kolliphor EL as surfactants and Transcutol HP as cosolvent was compared to a common oil vehicle, corn oil (CO). Serial dilutions of the pre-concentrates were performed in various media [distilled water and simulated intestinal fluids mimicking fasted state (FaSSIF) and fed state (FeSSIF)] and at different dilution ratios to simulate the *in vivo* droplets' behavior. The developed SNEDDS were assessed by means of phase separation, droplet size, polydispersity index, and  $\zeta$ -potential. Complex ternary diagrams were constructed to identify compositions exhibiting monophasic behavior, droplet size < 100 nm, and polydispersity index (PDI) < 0.25. Multifactor analysis and response surface areas intended to determine the factors significantly affecting droplet size. The oil capacity to accommodate lipophilic drugs was assessed *via* fluorescence spectroscopy based on the solvatochromic behavior of Nile Red. Solubility studies were performed to prepare fenofibrate- and itraconazole-loaded SNEDDS and assess their droplet size, whereas dissolution experiments were conducted in simulated intestinal fluids. Caco-2 cell viability studies confirmed the safety of the SNEDDS formulations at 1:100 and 1:1000 dilutions after cell exposure in culture for 4 h. The obtained results showed similar performance between RB and CO supporting the potential of RB as oil vehicle for the effective oral delivery of lipophilic compounds.

**KEY WORDS:** rice bran oil; SNEDDS; poorly soluble drugs; multifactor analysis; simulated intestinal fluids.

---

Guest Editor: Sanyog Jain

**Electronic supplementary material** The online version of this article (<https://doi.org/10.1208/s12249-018-1274-y>) contains supplementary material, which is available to authorized users.

<sup>1</sup>Laboratory of Pharmaceutical Technology, Department of Pharmacy, Aristotle University of Thessaloniki, 54124, Thessaloniki, Greece.

<sup>2</sup>Hellenic Agricultural Organization Demeter, Plant Breeding and Genetic Resources Institute, Thessaloniki, 57001, Thessaloniki, Greece.

<sup>3</sup>Hellenic Agricultural Organization Demeter, Cereal Institute, Thessaloniki, 57001, Thessaloniki, Greece.

<sup>4</sup>Laboratory of Pharmacology, School of Pharmacy, Aristotle University of Thessaloniki GR, 54124, Thessaloniki, Greece.

<sup>5</sup>To whom correspondence should be addressed. (e-mail: [dfatouro@pharm.auth.gr](mailto:dfatouro@pharm.auth.gr))

## INTRODUCTION

Safety, cost-effectiveness, and high patient compliance are the key elements that endorse oral drug delivery as the main route of administration of active pharmaceutical ingredients (APIs) (1,2). The majority of new synthesized chemical entities intended for oral administration are sparingly soluble compounds (1), classified as class II drugs in the Biopharmaceutics Classifications System (BCS) (3). To overcome the challenges of low aqueous solubility and low oral bioavailability of poorly soluble drugs, significant attention has been drawn on lipid-based drug delivery systems (LBDDS) (4,5) for which drug solubility in the gastrointestinal (GI) tract is crucial to enhance the dissolution performance and bioavailability properties of the formulation (6,7). The development of self-emulsifying drug delivery systems (SEDDS) is a formulation approach commonly adopted toward this direction (8,9).

SEDDS are isotropic mixtures which typically comprise of oils, surfactants, co-solvents, and the solubilized API. Self-nanoemulsifying drug delivery systems (SNEDDS) and self-microemulsifying drug delivery systems (SMEDDS) form nano- and microemulsions in aqueous media (e.g., GI fluids) under gentle agitation, with droplet sizes of approximately 60 and 100 nm, respectively (10,11). In general, preparation of SEDDS requires less energy, they are physically stable upon storage (12), and are easier to manufacture in large scale (13) compared to their lipid contenders (e.g., emulsions).

Incorporation of medium- and long-chain triglycerides as oil components in the formulation (corn oil (14–16), sesame oil (17–19); soybean oil (16,20,21); castor oil (16,22,23); olive oil (23–25); eucalyptus and orange oil (22); lemon and anise oil (26); peppermint oil (13,26); cinnamon and lavender oil (13)) is of critical importance in the preparation of SN/MEDDS. Both the type and amount of oil in the formulation composition significantly affect the API solubility in the carrier, the self-emulsification efficiency, and drug absorption *via* the GI tract (27,28). The surfactant content and the oil/surfactant ratio are additional formulation considerations requiring optimization to further improve the *in vitro*–*in vivo* performance of the formulation (29,30).

In the current study, we evaluated the effectiveness of rice bran (RB) oil as a drug carrier in SNEDDS preparation for the oral delivery of APIs exhibiting poor aqueous solubility. Exploitation of natural resources was the leading criterion in our study to investigate RB oil as a pharmaceutical excipient. RB is considered as a by-product of the rice milling process, while exhibiting a high nutritional value (proteins, lipids, fibers, vitamins, minerals) and antioxidant activity. (31). SNEDDS were also prepared with corn oil (CO) and their *in vitro* performance was compared to the respective containing RB (corn oil has been co-formulated in Neoral®, a marketed SNEDDS product). The performance of the drug-free formulations was assessed in different aqueous media after serial dilutions in distilled water (d.w.) and in simulated intestinal media [*i.e.*, fasted state simulated intestinal fluid (FaSSIF) and fed state simulated intestinal fluid (FeSSIF)] by means of visual inspection for phase separation, droplet size,  $\zeta$ -potential, and fluorescence spectroscopy. A multifactor analysis of variances (ANOVA) was performed to evaluate the effect of oil-, surfactant-, or cosolvent-related parameters on the droplet size, whereas Response Surface Methodology (RSM) was introduced as a supportive tool to plot the effect of the most significant interactions of factors. Fenofibrate (FENO) and itraconazole (ITRA) were loaded in selected formulations as model BCS class II compounds. FENO is medically used for its effects on the synthesis and catabolism of cholesterol and on triglyceride metabolism (32). FENO is a lipophilic prodrug ( $\log P = 5.24$ ) exhibiting poor aqueous solubility (33) and low oral bioavailability of its active metabolite (34). ITRA is used as a triazole antifungal agent for the treatment of infections such as histoplasmosis, blastomycosis, and refractory aspergillosis (35,36), presenting poor aqueous solubility (approximately 5  $\mu\text{g/ml}$  at pH 1 and 1  $\text{ng/ml}$  at pH 7) and high permeability (37). The dissolution properties of the tested drug-loaded formulations were assessed in simulated intestinal media and compared. To date, rice bran oil has been reported in the literature as excipient in the preparation of emulsion filled

gels (38) and oil-in-water emulsions (39). To the best of our knowledge, this is the first study reporting the use of rice bran oil as a drug carrier in the preparation of SNEDDS.

## MATERIALS AND METHODS

### Materials

Corn oil, fenofibrate, 3-(4,5-dimethylthiazol-2-yl)-2,5-diphenyltetrazolium bromide (MTT), and Triton X-100 and dimethyl sulfoxide (DMSO) were purchased from Sigma-Aldrich, Germany. A mixture of sodium taurocholate and soybean lecithin (SIF powder, Biorelevant.com, UK) was used in the preparation of FaSSIF and FeSSIF. Itraconazole was purchased from Fagron Hellas, Greece. Glycerol monolinoleate (Maisine CC) and diethylene glycol monoethyl ether (Transcutol HP) were kindly supplied by Gattefossé, France. Polyoxyl 40 hydrogenated castor oil (Kolliphor RH 40) and polyoxyl castor oil (Kolliphor EL) were kindly supplied by BASF, Germany. Dulbecco's modified Eagle's medium (DMEM), penicillin-streptomycin (10,000 U/mL), fetal bovine serum (FBS), MEM non-essential amino acids solution (100X), and phosphate-buffered saline 10X (PBS) were purchased from Gibco™ (Life Technologies, Grand Island, NY, USA). All other materials and reagents were of analytical grade. Deionized water (d.w.) was used in all experimental procedures.

### Rice Bran Oil Extract

Freshly harvested rice bran was stabilized under infrared heating, as previously described (31) and stored at  $-5^{\circ}\text{C}$ . RB oil extraction was performed using a single screw compression press machine at  $60^{\circ}\text{C}$  (40).

### Development of SNEDDS Preconcentrates

The tested formulations were Type IIIA systems in accordance with the Lipid Formulation Classification System (LFCS) (5). In detail, RB or CO oil (in 1:1 (*w/w*) mixtures with Maisine CC) were evaluated as oil vehicles. Kolliphor RH40 (RH) and Kolliphor EL (EL) were tested as hydrophilic surfactants to induce self-emulsification of the oil phase in the aqueous media. Transcutol HP (TR) was incorporated in the formulation as a cosolvent in order to increase the solubilization of the model lipophilic drug compounds. As a result, four different combinations were studied for each compound, namely, RB-RH, RB-EL, CO-RH, and CO-EL.

In each combination, the % *w/w* content of the oil phase (as 1:1 mixture of oil/Maisine CC), surfactant, and cosolvent in the formulations varied in the range of 51.0–67.8, 24.3–38.0, and 5.0–15.0% (*w/w*), respectively. In all cases, three factors were studied to formulate the SNEDDS preconcentrates: the type of oil, the oil-phase/surfactant ratio (1.5, 2.0, and 2.5), and the % (*w/w*) content of cosolvent (5, 10, and 15%). Therefore, nine different content combinations (*w/w*) were studied for each oil/surfactant combination, resulting in 36 compositions comprised of either RB or CO oil and RH or EL surfactant (Table I).

**Table I.** Composition of the Different SNEDDS Formulations (% w/w Content)

Sample	Oil <sup>a</sup> (% w/w)	Surfactant (% w/w)	Cosolvent (% w/w)	Oil/surfactant ratio
1	51.0	34.0	15	1.5
2	56.6	28.4	15	2.0
3	60.7	24.3	15	2.5
4	54.0	36.0	10	1.5
5	60.0	30.0	10	2.0
6	64.3	25.7	10	2.5
7	57.0	38.0	5	1.5
8	63.4	31.6	5	2.0
9	67.8	27.1	5	2.5

<sup>a</sup>The total oil phase content as 1:1 mixture of tested oils and Maisine CC

### Dilution of Preconcentrates in Aqueous Media

Since the *in vivo* performance of oral dosage forms is associated to the dilution of the drug carrier in the GI tract (5), all samples were diluted at three different ratios (*v/v*) (1:10, 1:100, and 1:1000) in three different aqueous media [d.w., FaSSIF, and FeSSIF], resulting in 324 samples.

### Dynamic Light Scattering and $\zeta$ -Potential Measurements

Dynamic light scattering (DLS) and  $\zeta$ -potential measurements were performed using a Malvern Nanosizer ZS, Malvern Instruments (UK). The droplet size, polydispersity index (PDI), and  $\zeta$ -potential values were recorded in triplicate and evaluated.

### Visual Inspection

All samples were visually inspected over a period of 24 h at ambient temperature to verify the miscibility of the components and to further clarify the compositions which resulted in monophasic dispersions. Samples exhibiting phase separation or blur dispersions were excluded from further studies.

### Construction of Ternary Phase-Size-Polydispersity Diagrams

The results obtained from visual inspection and DLS measurements were combined in ternary diagrams. The performance of each sample was evaluated based on certain assessment criteria defined for each parameter: monophasic behavior of the samples, droplet size <100 nm, and PDI < 0.25.

### Assessment of the Factors Affecting Droplet Size of SNEDDS

The obtained data from DLS measurements were processed in Minitab 17.1.0, Minitab Inc. to assess the effect of six independent factors and their interactions on the droplet size of the dispersed SNEDDS, through a multifactor ANOVA. The independent factors and their respective levels are presented at Table II. The studied system had 323 degrees of freedom. Evaluation of the effects and the significance level was projected in main effects and interactions plots.

RSM was complementary introduced to plot the response surface areas of the interactions of factors exhibiting significant alterations on droplet size.

### Fluorescence Spectroscopy

Fluorescence measurements were performed at ambient temperature using a Shimadzu RF-5301 fluorescence spectrophotometer. Two different compositions that fulfilled all criteria (phase-size-polydispersity) were chosen among the four oil/surfactant combinations. The preconcentrates were diluted at 1:100 ratio in d.w., FaSSIF, and FeSSIF, and mixed with the hydrophobic fluorescent stain Nile Red (NR) as a model drug at a final concentration of 26  $\mu$ M. NR was selected to assess the ability of oils to accommodate lipophilic compounds, due to its strong solvatochromic behavior and high affinity to lipid molecules (41). The excitation wavelength was set at 546 nm, the excitation and emission slit widths were both set at 1.5, and the emission spectra were recorded from 550 to 700 nm.

### Assessment of the Factors Affecting Fluorescence of NR

The obtained data from fluorescence measurements were analyzed using multivariate ANOVA as previously described, to evaluate the effects of oil type, surfactant type, % oil content, dilution medium, and their interactions on the fluorescence intensity of NR.

**Table II.** Summary of Factors and Their Levels Analyzed with Multivariate ANOVA

Factor	Levels	Values
Type of oil	2	RB, CO
Type of surfactant	2	RH, EL
Oil/surfactant ratio ( <i>w/w</i> )	3	1.5, 2.0, 2.5
Cosolvent (% <i>w/w</i> )	3	5, 10, 15
Dilution	3	1:10, 1:100, 1:1000
Medium	3	Water, FaSSIF, FeSSIF

### Quantification of the Active Compounds

Analysis of ITRA and FENO was performed using a high-performance liquid chromatography (HPLC) system, consisting of a LC-10 AD VP pump, a SIL-20A HT autosampler, and a UV-vis SPD-10A VP detector (Shimadzu), based on previously reported analytical conditions with modifications (42,43). HPLC analysis was carried out on a Discovery C18 column (150 mm, 4.6 mm, 5  $\mu$ m). The mobile phase consisted of acetonitrile/water (80:20 v/v; pH 2.5, adjusted with phosphoric acid) and was vacuum degassed and sonicated for 20 min before each measurement. The flow rate and injection volume were set at 1 mL/min and 30  $\mu$ L for FENO, whereas the respective values for ITRA were 0.7 mL/min and 40  $\mu$ L. FENO (retention time = 10.25 min) and ITRA (retention time = 6.26 min) were detected at 254 and 260 nm, respectively. Calibration curves of both APIs were linear over the range of 0.1–100  $\mu$ g/mL ( $R^2 \geq 0.999$ ).

### Solubility Studies and DLS of Drug-Loaded Formulations

The saturation solubilities of ITRA and FENO were determined in the four selected oil/surfactant SNEDDS combinations. An excess amount of each API was added at 2 mL of preconcentrate and kept under gentle agitation at ambient temperature. After 48 h, the samples were centrifuged at 10,000 rcf for 20 min to remove any undissolved residuals. Aliquots of the supernatants were filtered through PVDF 0.45  $\mu$ m filters, diluted in acetonitrile, and analyzed by HPLC.

Drug-loaded SNEDDS were prepared by adding an appropriate amount of each API to RB and CO samples containing either RH or EL. The final % content of the API in all formulations was equal to 80% of the saturation solubility of the sample. Alterations in the droplet size were assessed after dilution of selected drug-loaded formulations in aqueous media with DLS measurements performed as described above.

### Dissolution Studies

Hard gelatin capsules (size “0”) were filled with SNEDDS loaded with FENO or ITRA (600  $\mu$ L) to a final API content as described above (80% of the saturation solubility). Capsules were also filled with pure FENO or ITRA, to obtain an equivalent to the respective SNEDDS’ drug content. Dissolution studies were performed using a USP dissolution apparatus II (PT-DT7 Pharma Test AG, Germany) in 900 mL simulated intestinal fluid (SIF, 6.805 mg/mL;  $\text{KH}_2\text{PO}_4$ , 0.896 mg/mL NaOH; pH 6.8) at 75 rpm paddle rotation and 37°C. At predetermined time intervals, aliquots (1 mL) were withdrawn and replaced with fresh and preheated SIF. The samples were centrifuged at 4000 rcf for 15 min and filtered through PVDF 0.45  $\mu$ m filters. Appropriate dilutions in mobile phase were performed prior to HPLC analysis.

Furthermore, the release kinetics of the developed formulations were evaluated. Based on the obtained profiles, the dissolution data were fitted in two kinetic models, *i.e.*, first-order and Korsmeyer-Peppas (44), using SigmaPlot 12.5,

Systat Software Inc, and a curve fitting library (Release.jfl) provided by Systat Software Inc.

### Caco-2 Cell Cultures

Caco-2 cells (colon adenocarcinoma human cell line) were cultured in DMEM supplemented with 10% w/v FBS, 100 units/mL penicillin, 100 units/mL streptomycin, and 1x MEM non-essential amino acids and were incubated at 37°C in a humidified atmosphere with 5% v/v  $\text{CO}_2$ . Exponentially growing cells at passages between 42 and 45 were cultured *in vitro* to carry out the cellular viability assays.

### Cell Viability Assay

Caco-2 cell viability was evaluated after cell exposure to the SNEDDS formulations in a time- and concentration-dependent manner, using the MTT assay. Caco-2 cells were seeded in 96-well plates at a density of  $5 \times 10^4$  cells/well and were cultured for 48 h. Prior to treatment, the medium was removed and replaced by 100  $\mu$ L of the SNEDDS formulations diluted in HBSS at different ratios (1:10, 1:100, 1:1000). Cells treated with HBSS only were used as negative control and cells treated with 1% Triton X-100 were used as positive control. After treatment for 1, 2, and 4 h, the medium was replaced by 100  $\mu$ L MTT solution (0.5 mg/mL) and cells were further incubated for 3 h in a humidified atmosphere at 37°C. The MTT solution was carefully discarded and the formed formazan crystals were dissolved in 100  $\mu$ L DMSO. Absorbance was measured at 570 nm using an ELISA plate reader and cell viability was calculated according to the following equation:

$$\text{Cell viability (\% of control)} = \frac{\text{OD}_T - \text{OD}_B}{\text{OD}_C - \text{OD}_B} \times 100$$

where  $\text{OD}_T$ ,  $\text{OD}_B$ , and  $\text{OD}_C$  are the optical densities of the tested, blank, and control samples.

## RESULTS

### Droplet Size and $\zeta$ -Potential of Diluted Preconcentrates

The preconcentrates of RB or CO oil in mixtures with either RH or EL surfactants were diluted in various media and dilution ratios. A typical photo of RB-RH preconcentrates diluted in water is presented in Supplemental Information (Fig. S1), depicting visual changes in the color of the samples under simultaneous changes in the oil/surfactant ratio, dilution ratio, and % content of the cosolvent. The mean  $\pm$  SD values of droplet size, PDI, and  $\zeta$ -potential are presented at Table III. The minimum droplet size of the SNEDDS containing either RH or EL was approximately 30 nm, whereas a significant increase in the maximum droplet size of EL containing formulations was recorded at approximately 110–120 nm, compared to RH exhibiting maximum at approximately 90 nm for both oils. Typical size distribution graphs (by intensity) of RB-RH SNEDDS diluted at 1:100 (v/v) in water and at 1:1000 (v/v) in FeSSIF are presented in Fig. 1. Most of the SNEDDS/media/dilution combinations

**Table III.** Droplet Size and  $\zeta$ -Potential Values of the Oil-Surfactant Groups

Composition	Size (nm) <sup>a</sup>	PDI <sup>a</sup>	$\zeta$ -potential (mV) <sup>a</sup>
RB-RH	53.4 ± 11.5	0.16 ± 0.11	-6.2 ± 3.3
CO-RH	51.6 ± 10.3	0.15 ± 0.11	-6.5 ± 3.6
RB-EL	51.3 ± 16.1	0.21 ± 0.13	-7.4 ± 4.0
CO-EL	50.8 ± 16.5	0.21 ± 0.12	-7.8 ± 4.1

<sup>a</sup> Data are expressed as mean values ± SD ( $n=3$ )

exhibited PDI < 0.2 and narrow size distributions. However, in most cases, the samples diluted at 1:1000 ( $v/v$ ) in FeSSIF exhibited PDI > 0.25 and broad distributions. Insignificant alterations were observed in the surface charge measurements of SNEDDS ( $t$  test,  $p > 0.05$ ), independently of the parameters on study, with  $\zeta$ -potential values varying from -6.2 to -7.8 mV. The DLS measurements were further utilized in the construction of ternary diagrams and the effect of each factor on droplet size is further analyzed below.

### Visual Inspection of Phase Behavior

The produced SNEDDS preconcentrates were assessed as monophasic or phase separated in a period of 24 h to verify the miscibility of the components. Most of the compositions were identified as monophasic. In the case of phase separation, a distinct interface between the two separated phases could be easily observed. Typical monodisperse and phase-separated RB-RH samples are presented in Fig. 2. These results were further utilized in the construction of ternary diagrams, in combination with DLS data.

### Construction of Ternary Diagrams

The obtained data from visual inspection and DLS measurements were fitted in ternary diagrams to determine the acceptable samples simultaneously fulfilling the phase-

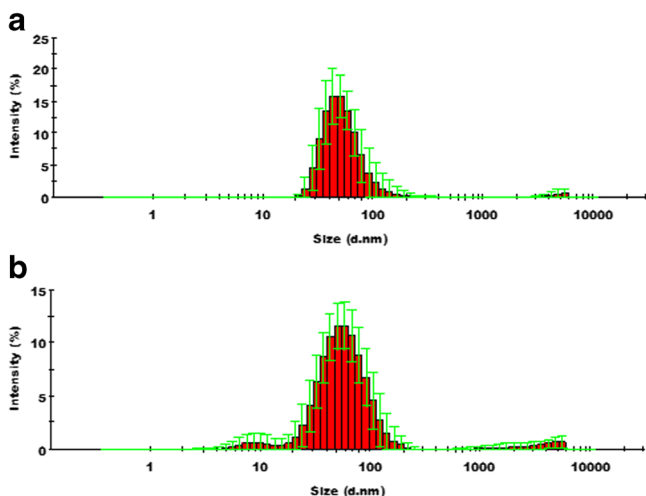


**Fig. 1.** Typical size distribution graphs (by intensity) of rice bran oil and Kolliphor RH 40 samples diluted **a** 1:100 ( $v/v$ ) in d.w. and **b** 1:1000 ( $v/v$ ) in FeSSIF. The droplet size and PDI were  $46.3 \pm 6.3$  nm and  $0.088 \pm 0.036$  for **a** and  $45.3 \pm 6.9$  nm and  $0.294 \pm 0.063$  for **b**, respectively

size-polydispersity criteria. In these diagrams, each criterion was illustrated as a distinct region-colored line to propose a common region where all set criteria are met. Consequently, the % content of optimal formulations was determined. The ternary diagrams presented a similar behavior between RB and CO in mixtures with either RH or EL (Fig. 3). The optimal area in the case of RH presented five common compositions between RB and CO (Fig. 3a, b), while the addition of EL resulted in four common compositions between the tested oil vehicles (Fig. 3c, d).

### Assessment of the Factors Affecting Droplet Size

ANOVA analysis was performed to define the main factors or their interactions that significantly affect the droplet size. The effect of the main factors (oil, surfactant, oil/surfactant ratio, cosolvent content, dilution ratio, medium) and their second-order interactions were assessed as critical at the significance level of 0.05.

The analysis of the main factors revealed a remarkable effect of the surfactant type ( $p = 0.034$ ), the oil/surfactant ratio ( $p < 0.001$ ), the % content of the cosolvent ( $p < 0.001$ ), and the type of dilution medium ( $p < 0.001$ ), while the oil type and dilution ratio did not present a significant effect on the droplet size ( $p = 0.105$  and  $p = 0.103$ , respectively). The main effects plot on droplet size is presented in Fig. 4.

Although individual variations in the main factors resulted in significant effects on the droplet size, deeper effects exist due to simultaneous changes on the level values of two factors. The second-order interactions plot *versus* droplet size is presented in Fig. 5.

Despite the insignificant effect of the type of oil on droplet size, the interaction of oil type and the % content of cosolvent were found to be considerable ( $p = 0.001$ ). Similar droplet size values were obtained for both oils at a 5% cosolvent content; however, at 10 and 15% content, the droplet size of rice bran oil compared to corn oil varied.

Significant interactions were also observed between the surfactant type and oil/surfactant ratio ( $p < 0.001$ ), cosolvent content ( $p < 0.001$ ), dilution ratio ( $p = 0.004$ ), and dilution media ( $p = 0.001$ ). In all cases, the use of RH or EL surfactants induced alterations on the droplet size of the SNEDDS formulations.

The droplet size trend was significantly altered at 1.5 and 2.5 oil/surfactant ratios when the cosolvent content varied from 5 to 15%, while a pronounced increase in the droplet size was observed upon interaction with the dilution media when the oil/surfactant ratio increased from 1.5 to 2.5.

Despite the insignificant alterations of the dilution ratio as a main factor, variations of significance were observed in the interaction between the dilution ratio and the type of medium ( $p < 0.001$ ). In FaSSIF media, increasing the dilution ratio from 1:10 to 1:1000 ( $v/v$ ) resulted in a gradual decrease in the droplet size, whereas this trend was reversed in d.w.

Response surface methodology was introduced in the analysis process to provide a better comprehension of the interaction between the oil/surfactant ratio and the % content of the cosolvent, as these factors showed the most significant effect on the droplet size. Additionally, the construction of the response surface areas provided a better visualization and comparison of the two studied oil vehicles and their effect on

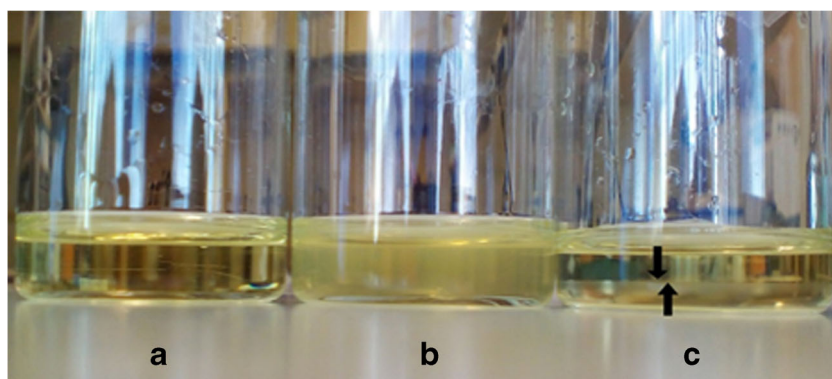


**Fig. 2.** Typical preconcentrates of SNEDDS that exhibit **a** a clear monophasic dispersion, **b** a turbid sample with phase separation after gentle agitation, and **c** a distinct interface between separated phases

the droplet size. The response surface areas are presented in Fig. 6. The response surface methodology was performed for the different types of oils and surfactants, while the SNEDDS formulations were diluted at 1:100 ratio in d.w. The dilution ratio of 1:100 presented the least significant droplet size alterations when the SNEDDS formulations were diluted in either d.w., FaSSIF, or FeSSIF media, compared to the 1:10 and 1:1000 ( $v/v$ ) dilution ratios (Fig. 6).

In the case of RH, both RB ( $R^2=0.953$ ) and CO ( $R^2=0.975$ ) presented a similar tendency to alter the SNEDDS droplet size depending on the oil/surfactant ratio and the % content of the cosolvent. Negligible alterations were observed for the oil/surfactant ratio of 1.5 when the cosolvent

content increased from 5 to 15%. However, the increase of cosolvent content resulted in a gradual reduction of the droplet size for the oil/surfactant ratio of 2.0 and this effect was more pronounced at the oil/surfactant ratio of 2.5. The effect of increasing the oil/surfactant ratio was more significant when the cosolvent content decreased from 15 to 5%.

The same behavior was observed for RB ( $R^2=0.763$ ) and CO ( $R^2=0.849$ ) when EL was introduced as the surfactant. The response surface areas revealed that the SNEDDS' droplet size was mainly dependent on the oil/surfactant ratio, while the cosolvent content did not show a significant effect.

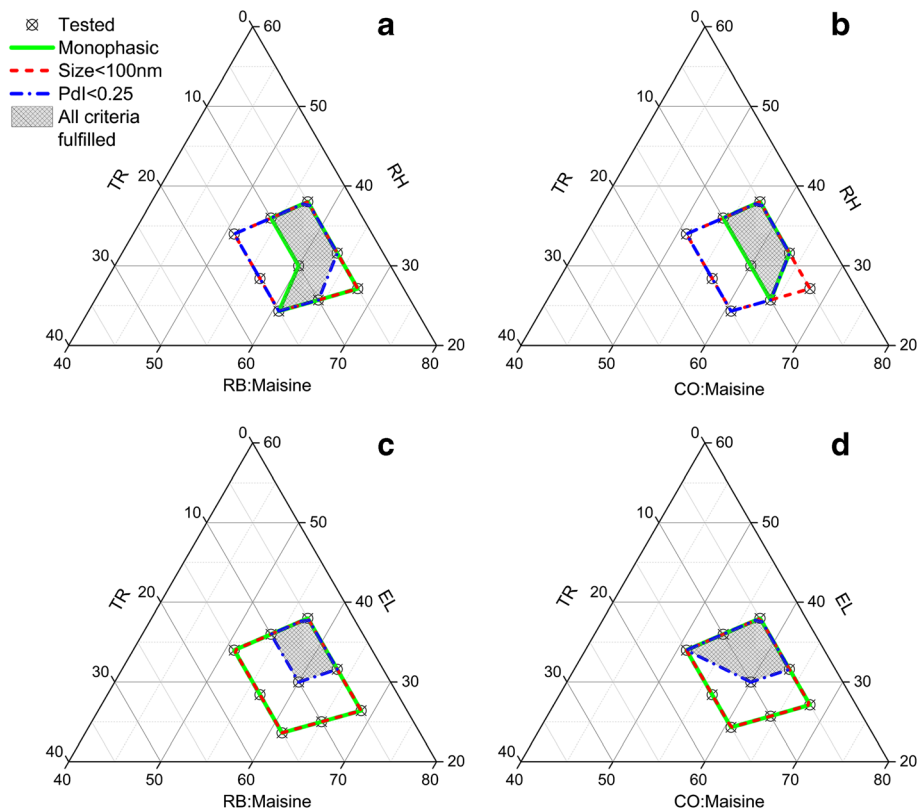


**Fig. 3.** Ternary phase-size-polydispersity diagrams, presenting the comparison between rice bran oil and corn oil, after the addition of surfactant Kolliphor RH 40 (**a** and **b**) or Kolliphor EL (**c** and **d**)

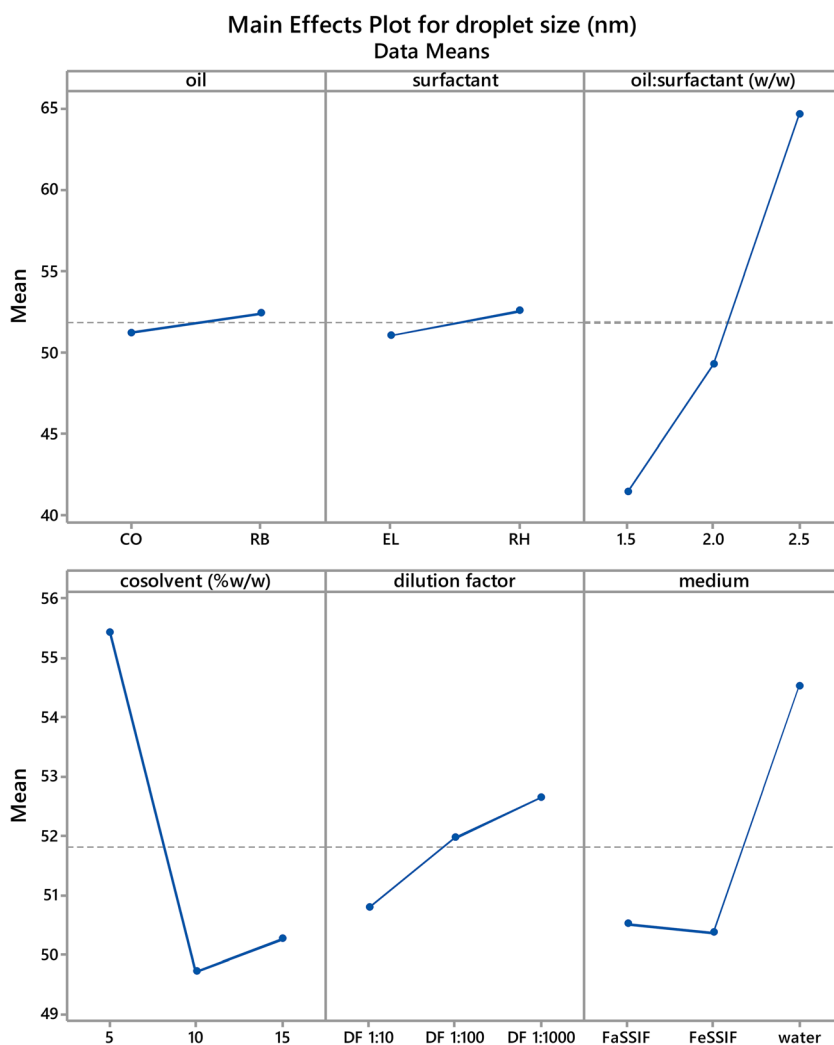


**Fig. 4.** Main effects plot on the droplet size of SNEDDS formulations

### Fluorescence Spectroscopy

The fluorescence spectra of the oil/surfactant combinations (Fig. 7) were recorded for two different oil contents (their composition is referred at Table III as samples 5 and 8) and the solvatochromic behavior of NR was monitored. Both samples were chosen since they fulfilled all set criteria and exhibited different % composition. In all cases, it was clear that the samples containing 63.4% oil phase exhibited higher fluorescence intensity compared to the respective containing 60% oil content. A reduction in the fluorescence intensity was observed when the micelle concentration in the dilution medium increased. The highest fluorescence intensity was evidenced in d.w. dilutions, whereas samples diluted in FeSSiF exhibited the minimum intensity.

### Assessment of the Factors Affecting NR Fluorescence

The fluorescence measurements were further supported by multivariate analysis and the main effects and the second-order interactions plots are demonstrated in Figs. 8 and 9, respectively. The oil and surfactant types were found to insignificantly alter the fluorescence intensity ( $p=0.465$  and

$p=0.908$ , respectively). Moreover, the % content of oil and the type of dilution media exhibited notable effects on the intensity of NR ( $p=0.011$  and  $p<0.001$ , respectively). The effect of second-order interactions between the four main factors on the fluorescence intensity was indicated as insignificant ( $0.086 < p < 0.341$ ).

### Solubility Studies and DLS Measurements

The saturation solubility of FENO and ITRA in samples comprised of either RB or CO as oil vehicles and RH or EL as surfactants was determined for the composition of sample 5 (Table III). In the case of FENO, superior performance of RB-RH and RB-EL samples compared to CO-RH and CO-EL was evidenced, exhibiting solubility values of  $130.76 \pm 1.52$ ,  $124.16 \pm 1.24$ ,  $119.23 \pm 1.35$ , and  $112.29 \pm 1.14$  mg/mL, respectively. Regarding ITRA, a reversed tendency was observed, as the saturation solubility of RB-RH and RB-EL was  $1.37 \pm 0.01$  and  $1.38 \pm 0.01$  mg/mL, whereas CO-RH and CO-EL presented solubility values of  $1.83 \pm 0.02$  and  $1.94 \pm 0.02$  mg/mL, respectively.

Drug-loaded formulations exhibiting the composition of sample 5 (Table III) were prepared in a final content of

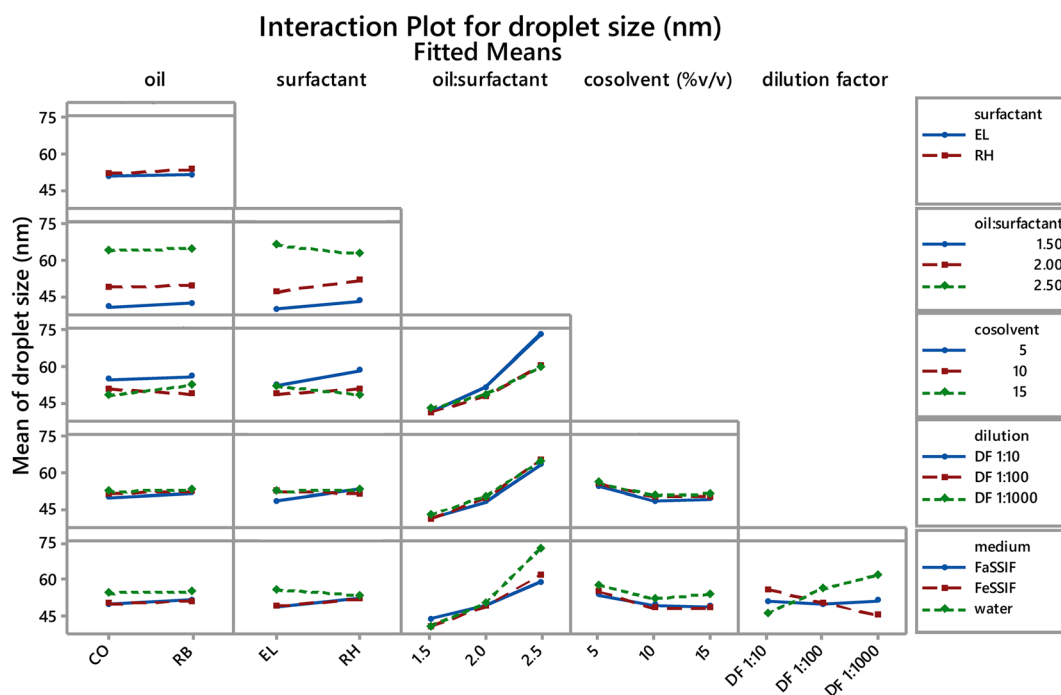


**Fig. 5.** Full interactions plot on the droplet size

either 90 mg/mL for FENO or 1.1 mg/mL of ITRA. DLS measurements were performed to determine the droplet size of formulations diluted in d.w., FaSSIF, and FeSSIF and dilution ratios of 1:10, 1:100, and 1:1000. Similarities on the scale of mean droplet size values, compared to drug-free formulations, were observed. As evidenced in Supplemental Information (Figs. S2–S3), the incorporation of active compounds in SNEDDS resulted in mean droplet size in the range 38.4–64.9 and 38.7–65.8 nm for FENO- and ITRA-loaded samples, respectively.

### Dissolution Studies

The dissolution profiles of drug-loaded formulations were recorded for 120 min in SIF. Incorporation of the lipophilic compounds in SNEDDS significantly enhanced the dissolution properties of both FENO and ITRA (Fig. 10). Regarding the powder-filled capsules, only 6.6% of FENO and 1.6% of ITRA were dissolved in the medium at 45 min. Almost 100% of the active content was released from the SNEDDS formulations at the same period ( $p > 0.05$ ), whereas

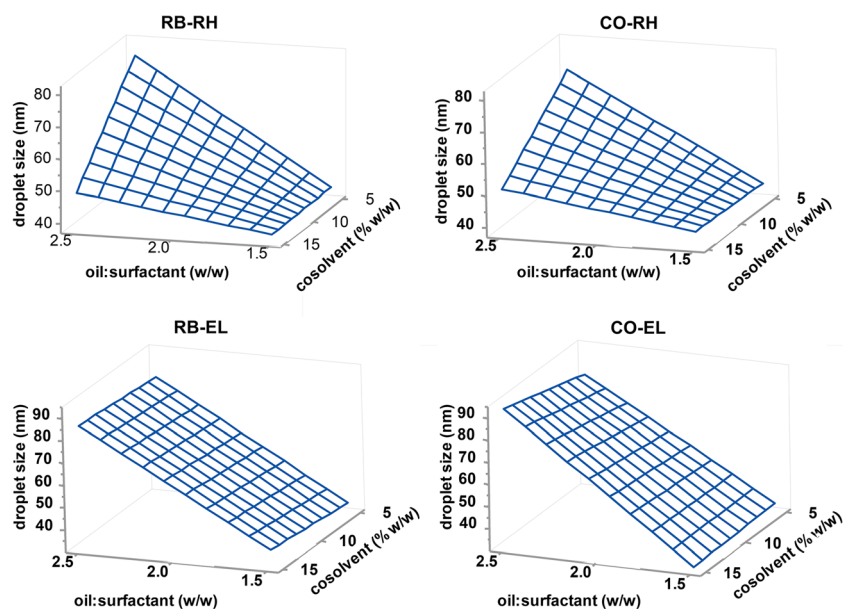


**Fig. 6.** Response surface areas of the various SNEDDS formulations, diluted in d.w. 1:100 (v/v)



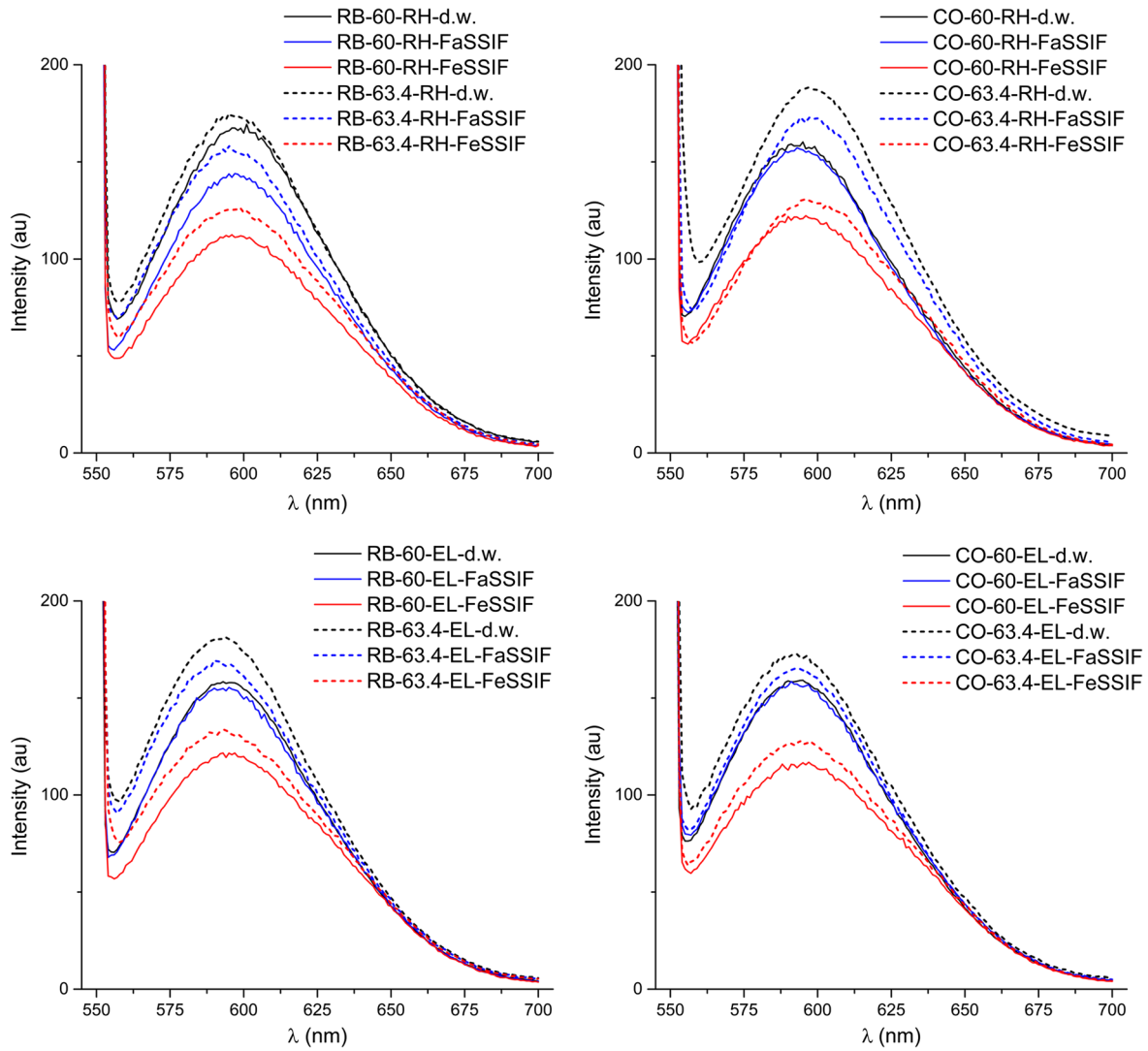


**Fig. 7.** Fluorescence spectra of the SNEDDS of samples 5 and 8, comprised of rice bran oil or corn oil, 60.0 or 63.4% total oil phase, Kolliphor RH 40, or Kolliphor EL as a surfactant and diluted 1:100 in d.w., FaSSIF, or FeSSIF

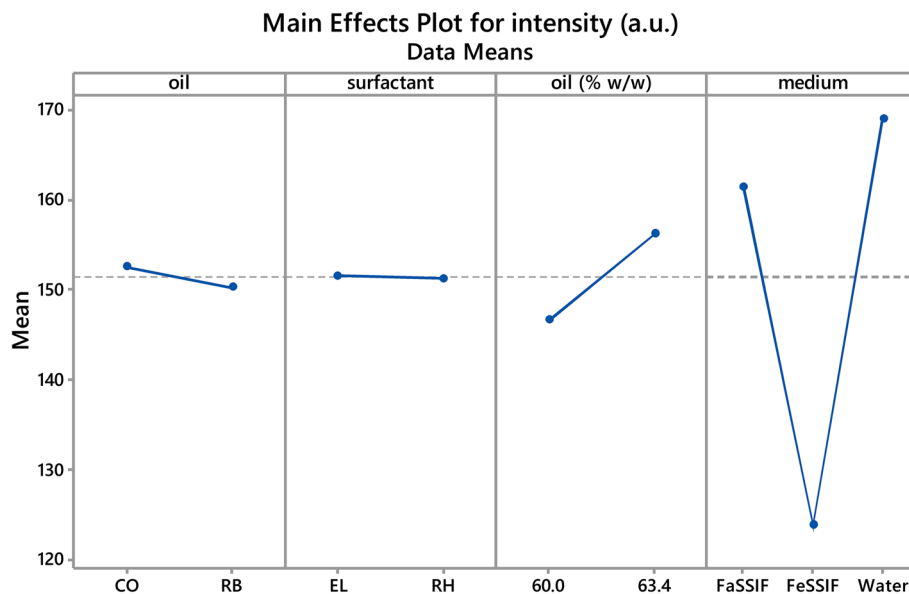


**Fig. 8.** Main effects plot on the fluorescence intensity of Nile Red

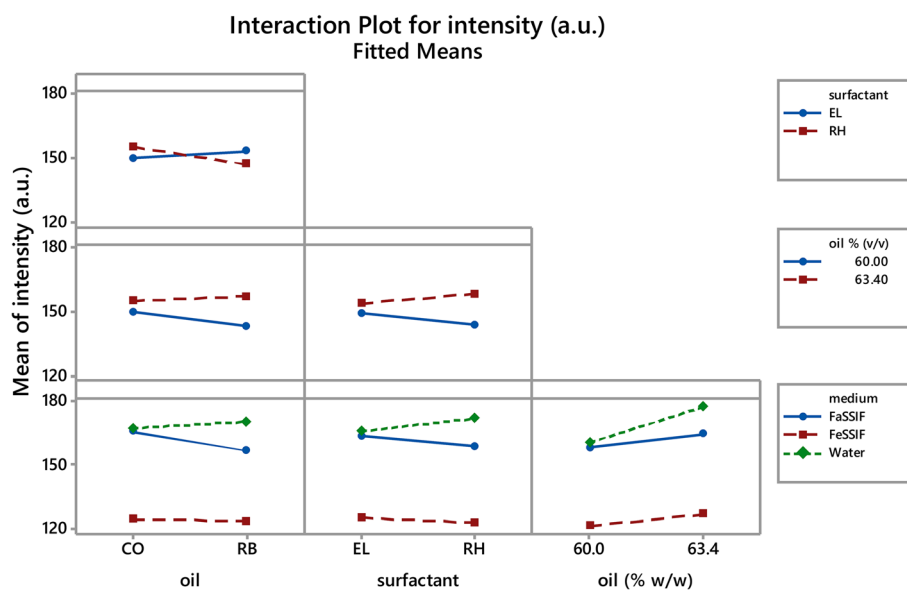


**Fig. 9.** Full interactions plot on Nile Red fluorescence

at the end of the experiment, the total amount of pure FENO and ITRA released was 11 and 4%, respectively.

The equation parameters ( $k$ ,  $n$ ) and square correlation coefficients ( $R^2$ ) of kinetic models applied in dissolution profiles of the developed formulations are presented at Table IV. Fitting the dissolution data of all formulations in Korsmeyer-Peppas equation resulted in  $R^2$  values in the range 0.8783–0.9370, for both ITRA and FENO. Optimal curve fitting was identified in the case of first-order kinetics, since  $R^2$  obtained values in the range 0.9778–0.9967.

#### Evaluation of Caco-2 Cell Viability *In Vitro* Following Exposure to SNEDDS Formulations

The cell viability of the SNEDDS formulations at different dilutions was evaluated in Caco-2 cells in a time-dependent manner using the MTT assay (Fig. 11). Caco-2 cell viability exceeded 80% following exposure to all SNEDDS formulations at dilutions of 1:100 and 1:1000 and at all time-points tested. However, a significant cytotoxic effect was

observed at 1:10 dilution for all SNEDDS formulations, which has been increased over time.

## DISCUSSION

### Droplet Size and $\zeta$ -Potential of SNEDDS

Since the self-emulsification process occurs when the SNEDDS pre-concentrates interact with GI fluids, the DLS studies were performed in d.w., FaSSiF, and FeSSiF. Alterations on the DLS measurements of SNEDDS were recorded, with respect to the tested parameters. The results were statistically analyzed in an attempt to clarify the effect of factors that significantly affected the droplet size. Upon initial inspection, a clear observation on PDI variations was evidenced in the case of diluted samples in FeSSiF. The graphs presented at Fig. 11 refer to RB-RH formulations diluted at 1:100 ratio in d.w. and at 1:1000 ratio in FeSSiF. Although both measurements resulted in well-defined populations of approximately 45 nm droplet size, a secondary

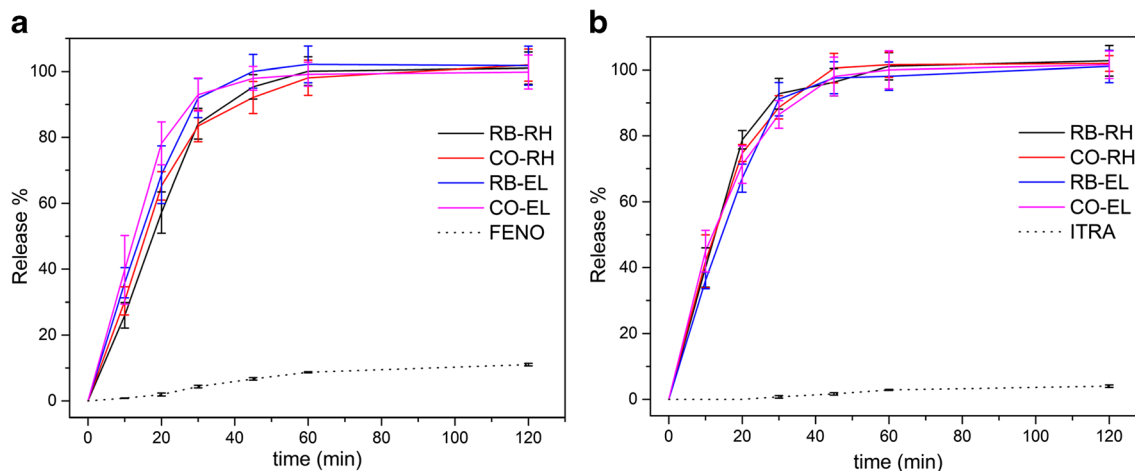


**Fig. 10.** Dissolution profiles of **a** fenofibrate and **b** itraconazole

**Table IV.** Release Kinetics of Itraconazole and Fenofibrate from Rice Bran and Corn Oil Formulations

Sample	ITRA					FENO				
	First-order		Korsmeyer-Peppas			First-order		Korsmeyer-Peppas		
	$k$	$R^2$	$k$	$n$	$R^2$	$k$	$R^2$	$k$	$n$	$R^2$
RB-RH	0.0684	0.9827	33.9803	0.2533	0.9074	0.0481	0.9778	21.1658	0.3544	0.8783
CO-RH	0.0662	0.9891	33.2608	0.2578	0.9167	0.0512	0.9847	23.9241	0.3256	0.9082
RB-EL	0.0588	0.9815	28.9661	0.2854	0.8971	0.0610	0.9857	29.4649	0.2859	0.8895
CO-EL	0.0640	0.9967	32.9850	0.2562	0.9370	0.0681	0.9833	35.0572	0.2429	0.8961

population of approximately 9 nm was identified in the FeSSIF size distribution graph, resulting in a threefold increase of the PDI value (PDI > 0.25).

It is worth mentioning that FeSSIF and FaSSIF media contain mixed micelles of *ca.* 6 nm and nanoparticles of *ca.* 60 nm (45) that potentially affect the scattering intensity and the PDI values in DLS measurements. Surprisingly, the nanoparticles in FaSSIF measurements coexisted with the same size-scaled SNEDDS droplets; thus, their presence was not recorded. Nevertheless, the presence of micelles in FeSSIF medium was clearly observed at 1:1000 dilution, as the content ratio of SNEDDS droplets to medium micelles was minimized, thus minimizing their interference on the measurements.

Moderate  $\zeta$ -potential values of approximately  $-7$  mV were recorded for both RB and CO SNEDDS, independently of the variable levels of the other studied factors. The potential impact of the droplets' surface charge on the long-term stability of the formulations is of great importance. However, aggregation was only observed in a limited number of samples as shown in the size distribution graph of Fig. 11,

due to the inadequate repulsion forces between the droplets (46).

### Visual Inspection of Phase Separation

The ability of RB oil to form monophasic dispersions was evaluated by visual inspection of the samples, in comparison to the respective preconcentrates formulated with CO. To ensure the exclusive identification of monophasic dispersions, samples presenting uncertain behavior were gently agitated. Phase separated samples instantly became turbid, as shown in Fig. 11 (sample B). Complementary to DLS measurements, the visual observations were imprinted in ternary diagrams, to facilitate identification of the best performing compositions.

### Construction of Ternary Diagrams

The construction of ternary phase-size-polydispersity diagrams is essential, to facilitate the selection of optimal SNEDDS. In addition to the monophasic behavior of samples and the droplet size criterion, PDI values in the range 0.1–

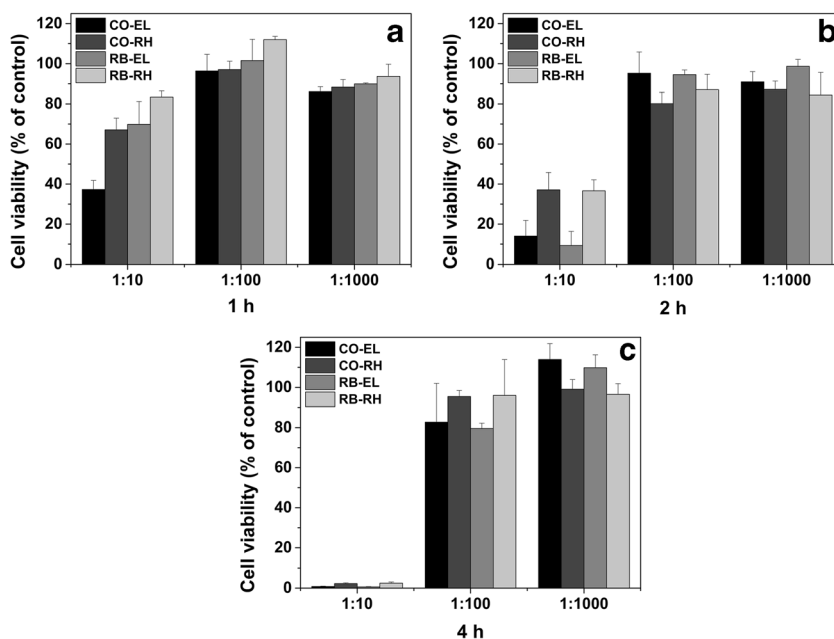


**Fig. 11.** Caco-2 cell viability was evaluated using the MTT assay following exposure of cultures to the SNEDDS formulations at different dilutions (1:10, 1:100, 1:1000) for **a** 1 h, **b** 2 h, and **c** 4 h. Data are presented as mean values  $\pm$  standard deviation ( $n = 3$ )

0.25 are indicative of a narrow size distribution, whereas values greater than 0.5 indicate a broad distribution (47). Although an array of measurements reported PDI values greater than 0.25, most of the related samples were diluted at 1:1000 in FeSSIF. Considering the presence of mixed micelles as analyzed above, the 1:1000 dilutions in FeSSIF were excluded from the assessment procedure on the selected criterion. As similar results were obtained from the comparison of fulfilled criteria and the optimal areas derived from the ternary diagrams, RB oil was characterized as an equal candidate on the development of SNEDDS, whereas alterations on the optimal areas were noticed upon incorporation of different surfactant types.

### Assessment of Factors Affecting Droplet Size

The multifactor analysis demonstrated similar effects of the tested oils on droplet size, as expected by the results of DLS measurements and the criteria restrictions of optimal areas in ternary diagrams. Droplet size is related to the available interfacial area between oil and aqueous phase, thus affecting the dissolution performance of drug-loaded formulations (10). Moreover, in the case of APIs where the dissolution rate is the limiting factor in drug absorption, enhancement of the *in vivo* performance is most likely to be achieved *via* strategic optimization of the SNEDDS' globule size (10,48).

Since serial dilutions occur during the *in vivo* administration of an oral dosage form, uniformity of the diluted emulsion and drug precipitation may critically affect drug release and the bioavailability of SNEDDS (49). The different dilution factors had no effect on the droplet size. This finding is indicative of the *in vivo* stability of the developed SNEDDS, as high dilutions of 1:100–1:1000 ratio simulate the final dilutions taking place in the GI tract, whereas the low dilution of 1:10 is most likely to promote drug precipitation (50).

Contrariwise, the effects of all surfactant-related main factors and interactions were considered significant. From a chemical point of view, the incorporation of surfactants with different hydrophilic–lipophilic balance (HLB) values would possibly alter the size distribution characteristics of the dispersion. RH is produced from the reaction of hydrogenated castor oil with ethylene oxide at a molar ratio of 1:40, while EL is produced by reacting castor oil with ethylene oxide at a molar ratio of 1:35 (51). The HLB values for these surfactants are in the range 14–16 and 12–14, respectively (data acquired from the technical data sheets of the surfactants Kolliphor RH40 and Kolliphor EL, BASF). The response surface areas complemented the evaluation process of RB. The tendency of droplet size to increase with simultaneous increase of the oil/surfactant ratio and decrease of the % cosolvent was identical between RB and CO oil, under incorporation of either RH or EL as surfactants. Without doubt, the overall assessment of the statistical analysis on droplet size confirmed that RB oil has the potential to replace CO oil in the studied formulations.

### Fluorescence Spectroscopy

The solvatochromic behavior of the lipophilic compound NR was employed to evaluate RB as a promising drug carrier

in SNEDDS formulations. The increase in fluorescent intensity of formulations with increasing the oil/surfactant ratio demonstrated the ability of RB to host and protect the lipophilic NR from the polar aqueous environment. Reduction of the fluorescent intensity was also observed when the micelle concentration in the dilution medium was increased. This is possibly attributed to the distribution of NR molecules in either the SNEDDS droplets or the micelle population; however, micelles are smaller in size than the SNEDDS droplets. Since the fluorescent intensity is proportionally related to the size of the particles hosting the fluorescent dye (52), micelles should present the lowest fluorescence intensity. As a result, the observed fluorescence intensity for the samples diluted in d.w. was the highest, in contrast to the FeSSIF-diluted pre-concentrates which exhibited the lowest intensity (Fig. 11). Multifactor ANOVA further corroborated the fluorescence spectroscopy results, as the content of oil and type of dilution media were found to significantly affect the intensity of NR.

### Solubility Studies and DLS Measurements of Drug-Loaded Formulations

A 10% increase in the solubilization capacity of FENO-loaded SNEDDS containing either RH or EL was observed in RB oil samples, compared to CO samples. On the contrary, ITRA solubility in RB formulations demonstrated a 25 to 30% reduction compared to the respective CO samples. Another remarkable finding was the effect of the surfactants on solubility values. FENO-loaded samples containing RH showed higher solubilities compared to EL samples, for either RB or CO, whereas this observation was reversed in the case of ITRA. As also mentioned in the evaluation of droplet size, the different chemical characteristics of the tested surfactants are more likely associated with alterations in the solubilization capacity of the various oil-surfactant formulations.

DLS measurements revealed that diluted samples in various aqueous media and at different dilution ratios exhibited similar droplet sizes, compared to drug-free pre-concentrates. An increase in the droplet size might affect drug absorption, due to the reduced available interface area of the particles on the intestinal site (53). Hence, the absence of alterations on the droplet size of both RB and CO drug-loaded formulations further supported equal performance between the two oil vehicles.

### Dissolution Studies

Dissolution studies were performed to evaluate the *in vitro* performance of RB and CO formulations. The data presented in Fig. 11 confirmed the dissolution enhancing properties of RB-SNEDDS compared to pure APIs ( $p < 0.05$ ). Moreover, similar dissolution profiles were obtained for both RB and CO, while the incorporation of different surfactants did not alter the dissolution properties of the formulation.

The dissolution data of the developed formulations were fitted to the first-order and Korsmeyer-Peppas equations. The SNEDDS formulations followed first-order kinetics showing a constant reduction in the drug release rate, proportional to the amount of drug present in the formulation at each time point (44).

## Evaluation of Caco-2 Cell Viability Following Exposure to the SNEDDS Formulations

Cell viability results illustrate the safety profile of the emulsion formulations containing RB oil after short-term cell exposure *in vitro*. The latter coincides with the fact that many oral dosage forms consisting of corn oil, Cremophor EL, and Cremophor RH40 as drug-solubilizing excipients are already available in the market (54), further highlighting the potential application of RB oil as a safe drug solubilizer in lipid-based formulations.

## CONCLUSIONS

The current study focused on the evaluation of RB oil, as an effective drug carrier in SNEDDS preparations. The performance of RB was investigated in comparison to CO, an established excipient of an already marketed SNEDDS product. The obtained results confirmed this hypothesis, thus rendering RB a very competent excipient of formulations intended for the oral delivery of lipophilic drugs.

## ACKNOWLEDGEMENTS

The current work has received financial support within the project “Sustainable techno-economic solutions for the agricultural value chain” Waste-7-2015 topic H2020 690142 project (AGROCYCLE). Gattefosse (France) and BASF (Germany) are greatly acknowledged for the generously gifted formulation excipients.

**Publisher’s Note** Springer Nature remains neutral with regard to jurisdictional claims in published maps and institutional affiliations.

## REFERENCES

- Cherniakov I, Domb AJ, Hoffman A. Self-nano-emulsifying drug delivery systems: an update of the biopharmaceutical aspects. *Expert Opin Drug Deliv*. 2015;12(7):1121–33.
- Krohe M, Eek D, Mazar I, Horsfield A, Pompilus F, Friebe R, et al. Patient-reported preferences for oral versus intravenous administration for the treatment of cancer: a review of the literature. *Patient Prefer Adherence*. 2016;10:1609–21.
- Amidon GL, Lennernäs H, Shah VP, Crison JRA. Theoretical basis for a biopharmaceutical drug classification: the correlation of *in vitro* drug product dissolution and *in vivo* bioavailability. *Pharm Res*. 1995;12(3):413–20.
- Pouton CW. Lipid formulations for oral administration of drugs: non-emulsifying, self-emulsifying and ‘self-microemulsifying’ drug delivery systems. *Eur J Pharm Sci*. 2000;11:S93–8.
- Pouton CW. Formulation of poorly water-soluble drugs for oral administration: physicochemical and physiological issues and the lipid formulation classification system. *Eur J Pharm Sci*. 2006;29(3–4):278–87.
- Porter CJ, Charman WN. *In vitro* assessment of oral lipid based formulations. *Adv Drug Deliv Rev*. 2001;50(Suppl 1):S127–47.
- Porter CJH, Trevaskis NL, Charman WN. Lipids and lipid-based formulations: optimizing the oral delivery of lipophilic drugs. *Nat Rev Drug Discov*. 2007;6(3):231–48.
- Fatouros DG, Karpf DM, Nielsen FS, Mullertz A. Clinical studies with oral lipid based formulations of poorly soluble compounds. *Ther Clin Risk Manag*. 2007;3(4):591–604.
- Kang BK, Lee JS, Chon SK, Jeong SY, Yuk SH, Khang G, et al. Development of self-microemulsifying drug delivery systems (SMEDDS) for oral bioavailability enhancement of simvastatin in beagle dogs. *Int J Pharm*. 2004;274(1–2):65–73.
- Charman SA, Charman WN, Rogge MC, Wilson TD, Dutko FJ, Pouton CW. Self-emulsifying drug delivery systems: formulation and biopharmaceutical evaluation of an investigational lipophilic compound. *Pharm Res*. 1992;9(1):87–93.
- Bakandritsos A, Zboril R, Bouropoulos N, Kallinteri P, Favretto ME, Parker TL, et al. The preparation of magnetically guided lipid based nanoemulsions using self-emulsifying technology. *Nanotechnology*. 2010;21(5):055104.
- Constantinides PP. Lipid microemulsions for improving drug dissolution and oral absorption: physical and biopharmaceutical aspects. *Pharm Res*. 1995;12(11):1561–72.
- Balakumar K, Raghavan CV, selvan NT, prasad RH, Abdu S. Self nanoemulsifying drug delivery system (SNEDDS) of rosuvastatin calcium: design, formulation, bioavailability and pharmacokinetic evaluation. *Colloids Surf B Biointerfaces*. 2013;112:337–43.
- Qian J, Meng H, Xin L, Xia M, Shen H, Li G, et al. Self-nanoemulsifying drug delivery systems of myricetin: formulation development, characterization, and *in vitro* and *in vivo* evaluation. *Colloids Surf B Biointerfaces*. 2017;160:101–9.
- Park JH, Kim DS, Mustapha O, Yousaf AM, Kim JS, Kim DW, et al. Comparison of a revaprazan-loaded solid dispersion, solid SNEDDS and inclusion compound: physicochemical characterisation and pharmacokinetics. *Colloids Surf B Biointerfaces*. 2018;162:420–6.
- Khan AW, Kotta S, Ansari SH, Sharma RK, Ali J. Self-nanoemulsifying drug delivery system (SNEDDS) of the poorly water-soluble grapefruit flavonoid Naringenin: design, characterization, *in vitro* and *in vivo* evaluation. *Drug Deliv*. 2015;22(4):552–61.
- Christiansen ML, Holm R, Abrahamsson B, Jacobsen J, Kristensen J, Andersen JR, et al. Effect of food intake and co-administration of placebo self-nanoemulsifying drug delivery systems on the absorption of cinnarizine in healthy human volunteers. *Eur J Pharm Sci*. 2016;84:77–82.
- Fatouros DG, Deen GR, Arleth L, Bergenstahl B, Nielsen FS, Pedersen JS, et al. Structural development of self nano emulsifying drug delivery systems (SNEDDS) during *in vitro* lipid digestion monitored by small-angle X-ray scattering. *Pharm Res*. 2007;24(10):1844–53.
- Fatouros D, Nielsen F, Douroumis D, Hadjileontiadis L, Mullertz A. *In vitro*–*in vivo* correlations of self-emulsifying drug delivery systems combining the dynamic lipolysis model and neuro-fuzzy networks. *Eur J Pharm Biopharm*. 2008;69(3):887–98.
- Shahba AA-W, Mohsin K, Alanazi FK. Novel self-nanoemulsifying drug delivery systems (SNEDDS) for oral delivery of cinnarizine: design, optimization, and *in-vitro* assessment. *AAPS PharmSciTech*. 2012;13(3):967–77.
- Thomas N, Holm R, Müllertz A, Rades T. *In vitro* and *in vivo* performance of novel supersaturated self-nanoemulsifying drug delivery systems (super-SNEDDS). *J Control Release*. 2012;160(1):25–32.
- Fahmy UA, Ahmed OAA, Hosny KM. Development and evaluation of avanafil self-nanoemulsifying drug delivery system with rapid onset of action and enhanced bioavailability. *AAPS PharmSciTech*. 2015;16(1):53–8.
- Patel J, Patel A, Raval M, Sheth N. Formulation and development of a self-nanoemulsifying drug delivery system of irbesartan. *J Adv Pharm Technol Res*. 2011;2(1):9–16.
- Abo Enin HA, Abdel-Bar HM. Solid super saturated self-nanoemulsifying drug delivery system (sat-SNEDDS) as a promising alternative to conventional SNEDDS for improvement rosuvastatin calcium oral bioavailability. *Expert Opin Drug Deliv*. 2016;13(11):1513–21.
- Sha X, Wu J, Chen Y, Fang X. Self-microemulsifying drug-delivery system for improved oral bioavailability of probucol: preparation and evaluation. *Int J Nanomedicine*. 2012;7:705–12.
- Villar AMS, Naveros BC, Campmany ACC, Trenchs MA, Rocabert CB, Bellowa LH. Design and optimization of self-nanoemulsifying drug delivery systems (SNEDDS) for enhanced dissolution of gemfibrozil. *Int J Pharm*. 2012;431(1–2):161–75.

27. Nielsen FS, Petersen KB, Müllertz A. Bioavailability of probucol from lipid and surfactant based formulations in minipigs: influence of droplet size and dietary state. *Eur J Pharm Biopharm.* 2008;69(2):553–62.
28. Gershanik T. Self-dispersing lipid formulations for improving oral absorption of lipophilic drugs. *Eur J Pharm Biopharm.* 2000;50(1):179–88.
29. Brouwers J, Tack J, Lammert F, Augustijns P. Intraluminal drug and formulation behavior and integration in in vitro permeability estimation: a case study with amprenavir. *J Pharm Sci.* 2006;95(2):372–83.
30. Kataoka M, Yokoyama T, Masaoka Y, Sakuma S, Yamashita S. Estimation of P-glycoprotein-mediated efflux in the oral absorption of P-gp substrate drugs from simultaneous analysis of drug dissolution and permeation. *Eur J Pharm Sci.* 2011;44(4):544–51.
31. Irakli M, Kleisiaris F, Mygdalia A, Katsantonis D. Stabilization of rice bran and its effect on bioactive compounds content, antioxidant activity and storage stability during infrared radiation heating. *J Cereal Sci.* 2018;80:135–42.
32. Yun H-Y, Joo Lee E, Youn Chung S, Choi S-O, Kee Kim H, Kwon J-T, et al. The effects of food on the bioavailability of fenofibrate administered orally in healthy volunteers via sustained-release capsule. *Clin Pharmacokinet.* 2006;45(4):425–32.
33. Munoz A, Guichard JP, Reginault P. Micronised fenofibrate. *Atherosclerosis.* 1994;110:S45–8.
34. Najib J. Fenofibrate in the treatment of dyslipidemia: a review of the data as they relate to the new suprabioavailable tablet formulation. *Clin Ther.* 2002;24(12):2022–50.
35. Akkar A, Müller RH. Intravenous itraconazole emulsions produced by SolEmuls technology. *Eur J Pharm Biopharm.* 2003;56(1):29–36.
36. Thakkar HP, Khunt A, Dhande RD, Patel AA. Formulation and evaluation of Itraconazole nanoemulsion for enhanced oral bioavailability. *J Microencapsul.* 2015;32(6):559–69.
37. Shevchenko A, Bimbo LM, Miroshnyk I, Haarala J, Jelínková K, Syrjänen K, et al. A new cocrystal and salts of itraconazole: comparison of solid-state properties, stability and dissolution behavior. *Int J Pharm.* 2012;436(1–2):403–9.
38. Nourbehesht N, Shekarchizadeh H, Soltanzadeh N. Investigation of stability, consistency, and oil oxidation of emulsion filled gel prepared by inulin and rice bran oil using ultrasonic radiation. *Ultrason Sonochem.* 2018;42:585–93.
39. Piriyaarasath S, Juttulapa M, Sriamornsak P. Stability of rice bran oil-in-water emulsions stabilized by pectin–zein complexes: effect of composition and order of mixing. *Food Hydrocoll.* 2016;61:589–98.
40. Srikaeo K, Pradit M. Simple techniques to increase the production yield and enhance the quality of organic rice bran oils. *J Oleo Sci.* 2011;60(1):1–5.
41. Theodoropoulos D, Rova A, Smith JR, Barbu E, Calabrese G, Vizirianakis IS, et al. Towards boron neutron capture therapy: the formulation and preliminary in vitro evaluation of liposomal vehicles for the therapeutic delivery of the dequalinium salt of bis-nido-carborane. *Bioorg Med Chem Lett.* 2013;23(22):6161–6.
42. Cendejas-Bueno E, Cuenca-Estrella M, Gomez-Lopez A. A simple, sensitive HPLC-PDA method for the quantification of itraconazole and hydroxy itraconazole in human serum: a reference laboratory experience. *Diagn Microbiol Infect Dis.* 2013;76(3):314–20.
43. Fei Y, Kostewicz ES, Sheu M-T, Dressman JB. Analysis of the enhanced oral bioavailability of fenofibrate lipid formulations in fasted humans using an in vitro–in silico–in vivo approach. *Eur J Pharm Biopharm.* 2013;85(3):1274–84.
44. Costa P, Sousa Lobo JM. Modeling and comparison of dissolution profiles. *Eur J Pharm Sci.* 2001;13(2):123–33.
45. Nielsen FS, Gibault E, Ljusberg-Wahren H, Arleth L, Pedersen JS, Müllertz A. Characterization of prototype self-nanoemulsifying formulations of lipophilic compounds. *J Pharm Sci.* 2007;96(4):876–92.
46. Efiána NA, Mahmood A, Lam HT, Zupančič O, Leonaviciute G, Bernkop-Schnürch A. Improved mucoadhesive properties of self-nanoemulsifying drug delivery systems (SNEDDS) by introducing acyl chitosan. *Int J Pharm.* 2017;519(1–2):206–12.
47. Wu L, Zhang J, Watanabe W. Physical and chemical stability of drug nanoparticles. *Adv Drug Deliv Rev.* 2011;63(6):456–69.
48. Hong J-Y, Kim J-K, Song Y-K, Park J-S, Kim C-K. A new self-emulsifying formulation of itraconazole with improved dissolution and oral absorption. *J Control Release.* 2006;110(2):332–8.
49. Gupta S, Chavhan S, Sawant KK. Self-nanoemulsifying drug delivery system for adefovir dipivoxil: design, characterization, in vitro and ex vivo evaluation. *Colloids Surf Physicochem Eng Asp.* 2011;392(1):145–55.
50. Ditner C, Bravo R, Imanidis G, Kuentz M. A systematic dilution study of self-microemulsifying drug delivery systems in artificial intestinal fluid using dynamic laser light backscattering. *Drug Dev Ind Pharm.* 2009;35(2):199–208.
51. Barmalexis P, Grypioti A, Eleftheriadis GK, Fatouros DG. Development of a new aprepitant liquisolid formulation with the aid of artificial neural networks and genetic programming. *AAPS PharmSciTech.* 2018;19(2):741–52.
52. Jores K, Haberland A, Wartewig S, Mäder K, Mehnert W. Solid lipid nanoparticles (SLN) and oil-loaded SLN studied by spectrofluorometry and Raman spectroscopy. *Pharm Res.* 2005;22(11):1887–97.
53. Hussain MD, Mohsin K, Alamari R, Ahmad A, Raish M, Alanzi F. Development of self-nanoemulsifying drug delivery systems for the enhancement of solubility and oral bioavailability of fenofibrate, a poorly water-soluble drug. *Int J Nanomedicine.* 2016;11:2829–38.
54. Strickley RG. Solubilizing excipients in oral and injectable formulations. *Pharm Res.* 2004;21(2):201–30.